

Direct determination of exact charge states of surface point defects using scanning tunneling microscopy: As vacancies on GaAs (110)

Kuo-Jen Chao, Arthur R. Smith, and Chih-Kang Shih*
Department of Physics, University of Texas, Austin, Texas 78712
(Received 25 July 1995)

We show a direct determination of the charge state of surface As vacancies on *p*-type GaAs(110) using scanning tunneling microscopy. This method utilizes the compensation between the local band bending resulting from the As vacancy and the *p*-type dopant whose charge states are known *a priori*. Detailed analysis shows a one-to-one compensation between the dopant-related and As-vacancy-related features, indicating that the As vacancy has a charge of +1. This method can be extended to determine quantitative charge states of other point defects (positive or negative).

The subject of surface point defects has been a fruitful and challenging one in condensed-matter physics and the related physical sciences. Surface defects play critical roles in the surface kinetics of epitaxial growth, in surface electrical characteristics such as Fermi-level pinning and surface carrier recombination, and in other areas of surface science. For many years, researchers have tried to characterize the structural and chemical nature of these surface defects and have tried to determine their electronic properties such as their energy levels and quantitative charge states. Recently there has been significant progress in the identification of the structural and chemical nature of surface and subsurface point defects using scanning tunneling microscopy (STM).¹⁻¹⁰ For example, anion-antisite,¹ cation and anion vacancies,²⁻⁵ and substitutional dopant impurities^{6,7} on III-V compound surfaces and subsurfaces have been identified recently. In the case of the As-antisite defect,¹ tunneling spectroscopy has been used to identify the energy level of the defect. The focus of this paper is the quantitative determination of the charge states of surface point defects.

It has been well established that the sign of the charge state of a defect can be deduced from the long-range topographic distortion (LTD) as measured with the STM (by LTD, we are referring to the local background in the immediate vicinity of a defect upon which the atomic corrugations are superimposed in the STM images; this background may be hillock or a depression, depending on the charge of the defect, and typically has a lateral extent of many lattice constants).⁸ For example, a negatively charged defect such as oxygen on *n*-type GaAs (110) surfaces depletes local carrier density and creates local band bending, resulting in a depression having a lateral extent corresponding to the screening length (or Debye length) in empty-state images.⁹ This method has also been utilized to determine the sign of the charge of surface anion vacancies in III-V compounds.^{2,3} However, quantitative determination of charge states has been very difficult without having to rely upon theory.^{2,11} The main difficulties of utilizing the LTD to determine the magnitude of the charge state are first, that the magnitude of the LTD shows a strong bias dependence and second, that the tip electronic states are unknown in a typical STM experiment. For example, in the case of *n*-type dopants in GaAs whose charge state is known *a priori*, it has been shown that

the magnitude of the LTD can vary by more than a factor of ten over the bias range from 1.5 to 3.0 V.⁶ Nevertheless, it was possible for Pashley, Haberern, and Feenstra¹² to infer the magnitude of the charge state of the kink site on GaAs (001) by employing an effective-mass model and also by taking into account scattering from a Coulomb potential.

In this paper, we show a method that allows the direct determination of the charge states of surface point defects that requires no theoretical modeling. Using this method, we have determined that the charge state of the As vacancy on a *p*-GaAs (110) surface is +1, in contrast to recent work based on a theoretical calculation.² We now outline our method. Since an ionized acceptor dopant creates an attractive Coulomb potential for free carrier holes and a charged As-vacancy creates a repulsive Coulomb potential for free carrier holes, the sign of the LTD will be opposite for these two defects. Further, we know that the magnitude of the LTD is proportional to the charge density. As a result, filled-state images show ionized dopant atoms as hillocks and charged arsenic vacancies as depressions. In our method, we assume that the magnitudes of the LTD's for the dopants and the vacancies are comparable. We believe this assumption is valid since the measurement method in each case is identical, namely, the STM tip is sensing the concentration of free carrier holes. Further, when an acceptor atom and an arsenic vacancy are closed enough that the free-carrier density almost completely cancels out, we are left with just the structural deviation of the missing arsenic atom. We can then subtract this structural deviation from the LTD of the charged arsenic vacancy and compare this with the LTD of the ionized dopant atom. Since the charge state of the ionized dopant atom is known to be -1 *a priori*, we can then determine the numerical value for the charge of the arsenic vacancy. The basic principle of this method is general and can be implemented to determine the charge state of other surface point defects as well.

We also explain how our method avoids the two difficulties mentioned previously. First, it is certainly true that the LTD depends on the tip bias since this will determine the particular charge density contour followed by the tip. However, in our case, we simply image both dopants and vacancies with the same bias, which results in a common reference level for the LTD's. This allows us to make a direct compar-

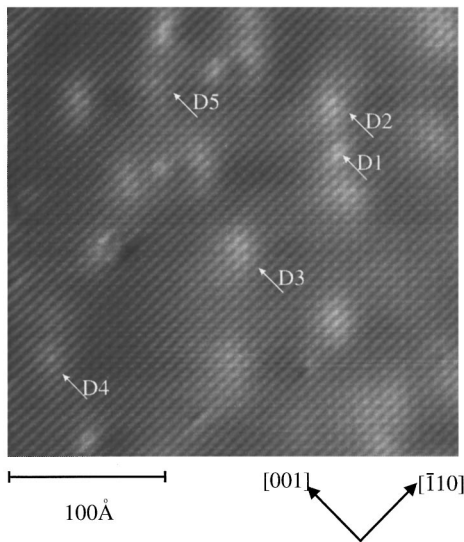


FIG. 1. A $300 \text{ \AA} \times 300 \text{ \AA}$ filled-state image acquired at a sample bias of -1.57 V and a tunneling current of 0.1 nA . Hillock features correspond to “observable” p -type dopants. Representatives of dopants in each layer are marked as $D1$ to $D5$. This image is not corrected for thermal drift.

son. Second, the tip electronic states certainly play a role in the STM image since the image is really a convolution of tip and sample electronic states. But in our case we use the same tip for imaging both the dopants and the vacancies; therefore, we do not need to consider the detailed electronic states of the tip. By imaging dopants and vacancies with the same tip at the same tip bias, we can directly compare the resulting LTD's and determine the charge states of surface point defects.

Our experiments were performed in a UHV-STM system (base pressure of $<4.5 \times 10^{-11}$ torr) described earlier.¹³ Tungsten tips were cleaned *in situ* using e -beam heating and/or field emission. Bridgman-grown p -type GaAs samples with Zn dopant levels of $4 \times 10^{19} \text{ cm}^{-3}$ were cleaved *in situ* to expose (110) surfaces. STM images were acquired at various locations on the surface with different surface As-vacancy concentrations.

Shown in Fig. 1 is a $300 \text{ \AA} \times 300 \text{ \AA}$ filled-state image acquired at a sample bias of -1.57 V and a tunneling current of 0.12 nA . The image corresponds to that of the As sublattice.¹⁴ In this image with very few defects one observes many hillock features that have been identified as p -type dopants recently by Johnson *et al.*⁷ Similar observations have been reported by Zheng *et al.*⁶ for n -type dopants. Detailed line profile analysis across those hillocks indicates that there are about five layers of dopant atoms being observed, similar to those described by Johnson *et al.*⁷ Representatives of dopants in each layer are marked as $D1$ to $D5$. The dopant counting yields a surface concentration of $3.3 \times 10^{12} / \text{cm}^2$ per five layers, corresponding to a bulk concentration of $3.3 \times 10^{19} / \text{cm}^3$ if one assumes that the concentration is uniformly distributed up to the surface layer. This number is in reasonable agreement with the given bulk dopant concentration. Shown in Fig. 2 is a $360 \text{ \AA} \times 360 \text{ \AA}$ filled-state image acquired at a sample bias of -2.45 V and a tunneling current of 0.1 nA at a different location. In addition to the dopant-

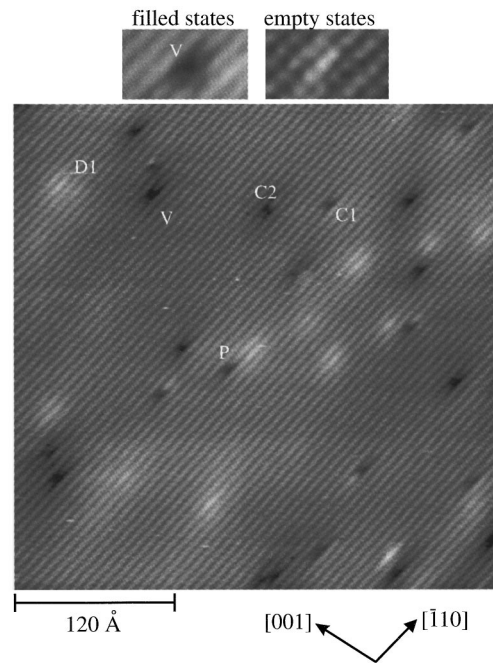


FIG. 2. A $360 \text{ \AA} \times 360 \text{ \AA}$ filled-state image acquired at a sample bias of -2.45 V and a tunneling current of 0.1 nA . The image is not corrected for thermal drift. One of the isolated As vacancies is marked as V ; one of the isolated dopants in the first layer is marked as $D1$; $C1$ marks the feature where the carrier depletion and carrier accumulation due to the vacancy and the dopant compensate each other almost completely; $C2$ is a feature where the dopant from a deeper layer is only partially compensated by the vacancy, leaving a long-range depression with magnitude smaller than that of an isolated As vacancy. The feature marked as P represents the partial compensation between the surface As vacancy and the dopant in the first layer. Shown in the inset are polarity-dependent images used to identify the isolated As vacancy acquired at $\pm 2.35 \text{ V}$ (following Ref. 2).

associated hillocks, one observes many missing lattice sites in this image, corresponding to As vacancies such as those described by Lengel *et al.*² Identification of single As vacancies is achieved by using dual-bias images such as those in which the filled-state image shows a missing As-lattice site while the empty-state image shows the two Ga-lattice sites next to this missing As-lattice site being raised. An example is shown in the inset. For an isolated As vacancy (one of them is marked as V), one observes a local depression in the apparent topography as a result of local band bending. In addition to isolated As vacancies, one more often observes areas where the local depression of the As vacancy and the local accumulation of the hillocks cancel or partially cancel each other. We refer to this as compensation. Such a compensation is also responsible for the smaller concentration of observable dopants in Fig. 2 when compared to those in Fig. 1. This compensation behavior and the *a priori* knowledge of the charge state of the dopant form the basis of our method for determining the quantitative charge states of the surface As vacancies.

We now discuss the compensation mechanism. Following the arguments of Johnson *et al.*⁷ and Zheng *et al.*,⁶ the p -type dopant atoms on an unpinned surface can be observed as the tip-induced band bending effectively creates a singly

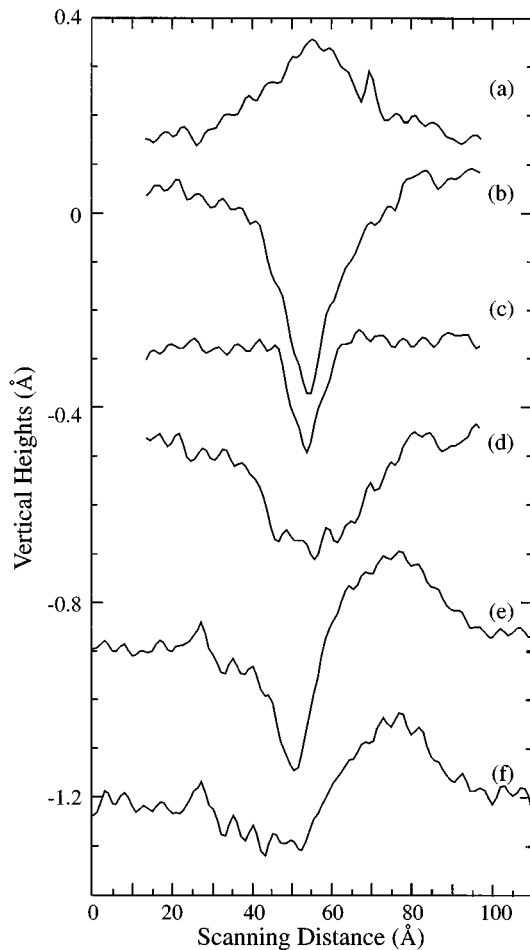


FIG. 3. Line profiles along the $[\bar{1}10]$ direction across various features of the image shown in Fig. 2. (a) Across the isolated dopant in the first layer $D1$; (b) across the isolated vacancy V ; (c) across the complete compensated feature $C1$; (d) the difference of (b)–(c); (e) across the P feature; (f) the difference of (e)–(c), representing the carrier depletion and accumulation across the atomic scale dipole P .

charged state (-1) on the acceptor impurities. The local Coulomb potential in turn attracts free carrier holes, resulting in hillocks being observed in the filled-state STM image. Shown in Fig. 3(a) is a line profile along the $[\bar{1}10]$ direction across such a dopant-related hillock feature (labeled as $D1$ in Fig. 2). Describing this with a hydrogenic mode, the Bohr radius of such a hillock feature is about 15 ± 3 Å. This profile corresponds to the dopant atom located in the first sublayer. Hillocks due to deeper dopants have smaller integrated area. Now consider an isolated arsenic vacancy. When the defect density is still low, the surface Fermi level (E_F) is near the valence-band maximum. In this case, the defect electronic states associated with the As vacancy are not occupied, resulting in a positively charged state whose magnitude is to be determined. This positively charged state repels free carrier holes, creating a local depression in the topographic image. Shown in Fig. 3(b) is a line profile along the $[\bar{1}10]$ direction across an isolated As vacancy (marked as V in Fig. 2). This line profile contains both the structural deviation from a perfect lattice and the effect of local band bending described

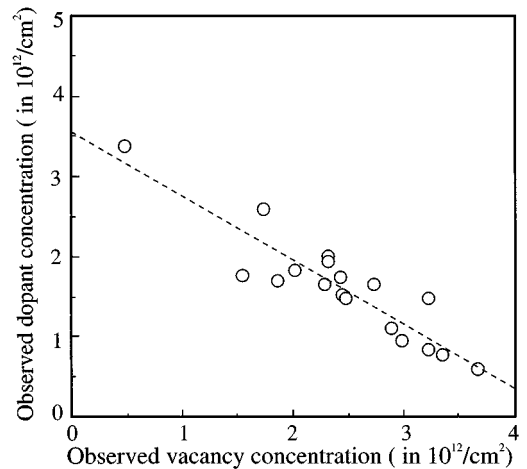


FIG. 4. Observed dopant concentration versus the observed vacancy concentration (labeled as open circles). The best-fit line for the dopant versus vacancy concentration has a negative slope of -0.8 , indicating that on the average, only 80% of the dopants are compensated by the vacancies. This result is consistent with the detailed analysis for Fig. 2.

above. The magnitude of the local band bending is directly related to the magnitude of the charge.

When a positively charged As vacancy (which repels free carrier holes) and a negatively charged dopant atom (which attracts free carrier holes) are very close to each other (within a few lattice constants), one expects to observe a form of compensation between these two features. For example, marked as feature $C1$ in Fig. 2, one sees a nearly complete compensation between the local depletion and accumulation of carriers. In this case, the STM topography contains only the structural deviation from a perfect lattice. Indeed, in the line profile along the $[\bar{1}10]$ direction shown in Fig. 3(c) the long-range depression is absent. Since line profile 3(b) contains both the electronic and the structural effects while the electronic effect in line profile 3(c) is completely compensated, the difference of the two line profiles, $3(d) = 3(b) - 3(c)$, represents the electronic effect due to the positively charged As vacancy only. When one compares profile 3(d) to the carrier accumulation profile near the dopant atom [3(a)], one finds that they are exactly reversed. The integrated areas below the two line profiles are 6.2 ± 0.5 and 5.8 ± 0.5 Å², respectively, essentially identical within the experimental error. This result indicates that the charge state of the As vacancy has to be $+1$. If the charge state of the As vacancy was $+2$ or higher, the magnitude of the local depression contour would have to be much greater.

In the case where the charged vacancy and ionized dopant atom are within one or two Bohr radii of each other, partial compensation is observed (marked as P in Fig. 2). The line profile along the $[\bar{1}10]$ direction is also shown in Fig. 3(e). Following a similar procedure to subtract the structural deviation, we obtain the resulting profile in 3(f), which clearly shows a reversal of charge accumulation to depletion. In essence, this is an atomic-scale “dipole” formed by the $+1$ charged As vacancy and the -1 charged dopant atom. The resulting profile can be fit very well by superposition of the accumulation and depletion profiles shown in 3(d) and 3(a)

with their centroids placed about 4 lattice sites apart along the $[110]$ direction. Again, this result indicates that the charge state of the As vacancy has to be +1, in contradiction to the recent theoretical calculation of +2 described by Lengel *et al.*²

Due to the large dopant concentration in our samples, for sheer statistical reasons most of the vacancies encounter dopant atoms nearby. Some of them compensate the dopants on the first layer such as feature C1 in the image, some of them compensate dopant features from deeper layers such as the feature marked as C2 in the image. In the image shown in Fig. 2, only 4 out of 22 vacancies do not compensate dopants at all. We further perform dopant and vacancy counting over a large number of images acquired on the same sample surface, and we find a large variation in the vacancy concentration. The result of the observed dopant concentration versus the observed vacancy concentration is shown in Fig. 4 (shown as open circles). Each data point is obtained from an area of at least $400 \text{ \AA} \times 400 \text{ \AA}$. The best-fit line for the dopant concentration versus the vacancy concentration yields a slope of -0.8 . If one assumes that the underlying dopant

concentration is constant, this result indicates that, on the average, only 20% of the arsenic vacancies are isolated.

In summary, we have demonstrated a method to directly determine the exact charge states of surface point defects using STM. The method relies on the compensation between the free carrier accumulation and depletion stemming from the ionized dopants and surface point defects. Since the charge states of the ionized dopants are known, such a compensation mechanism provides a means for quantifying the charge states of the surface point defects. By utilizing this procedure, we have determined that the charge state of an isolated As vacancy on *p*-type GaAs(110) is +1. The principle behind this method is rather general and can be extended to determine the quantitative charge states of other surface point defects. For example, quantification of negatively charged point defects can be achieved by using an *n*-type sample.

This work was partly supported by the National Science Foundation, Grant No. DMR-94-02938 and the Science and Technology Center Program of the National Science Foundation, Grant No. CHE8920120.

*Author to whom all correspondence should be addressed.

¹R. M. Feenstra, J. M. Woodall, and G. D. Pettit, *Phys. Rev. Lett.* **71**, 1176 (1993).

²G. Lengel, R. Wilkins, G. Brown, M. Weiner, J. Gryko, and R. E. Allen, *Phys. Rev. Lett.* **72**, 836 (1994).

³Ph. Ebert, K. Urban, and M. G. Lagally, *Phys. Rev. Lett.* **72**, 840 (1994).

⁴Ph. Ebert, G. Cox, U. Poppe, and K. Urban, *Ultramicroscopy* **42-43**, 871 (1992).

⁵G. Lengel, R. Wilkins, G. Brown, and M. Weiner, *J. Vac. Sci. Technol. B* **11**, 1472 (1993).

⁶J. F. Zheng, X. Liu, N. Newman, E. R. Weber, D. F. Ogletree, and M. Salmeron, *Phys. Rev. Lett.* **72**, 1490 (1994).

⁷M. B. Johnson, O. Albrektsen, R. M. Feenstra, and H. W. M. Salemink, *Appl. Phys. Lett.* **63**, 2923 (1993); **64**, 1454 (1994).

⁸J. A. Stroscio and R. M. Feenstra, in *Scanning Tunneling Microscopy*, edited by J. A. Stroscio and W. J. Kaiser, *Methods of Experimental Physics Vol. 27* (Academic, New York, 1993), pp. 95–147.

⁹J. A. Stroscio, R. M. Feenstra, and A. P. Fein, *Phys. Rev. Lett.* **58**, 1668 (1987).

¹⁰S. Gwo, A. R. Smith, and C. K. Shih, *J. Vac. Sci. Technol. A* **11**, 1644 (1993).

¹¹J. -Y. Yi, J. S. Ha, S. -J. Park, and E. -H. Lee, *Phys. Rev. B* **51**, 11 198 (1995).

¹²M. D. Pashley, K. W. Haberern, and R. M. Feenstra, *J. Vac. Sci. Technol. B* **10**, 1874 (1992).

¹³S. Gwo, K.-J. Chao, C. K. Shih, K. Sadra, and B. G. Streetman, *Phys. Rev. Lett.* **71**, 1883 (1993).

¹⁴R. M. Feenstra, J. A. Stroscio, J. Tersoff, and A. P. Fein, *Phys. Rev. Lett.* **58**, 1192 (1987).